1 **Microbiome and resistome profiles along a sewage-effluent-reservoir trajectory underline the role of**
2 **natural attenuation in wastewater stabilization reservoirs**

3 Inês Leão[b*], Leron Khalifa[a*], Nicolas Gallois[c*], Ivone Vaz-Moreira[b], Uli Klümper[d], Daniel Youdkes[a], Shaked
4 Palmony[e], Lotan Dagai[e], Thomas U. Berendonk[d], Christophe Merlin[c], Célia M. Manaia[b], and Eddie Cytryn[a]

5 [a] Institute of Soil, Water and Environmental Sciences, Volcani Institute, Agricultural Research
6 Organization, Rishon-Lezion, Israel.

7 [b] Universidade Católica Portuguesa, CBQF - Centro de Biotecnologia e Química Fina – Laboratório
8 Associado, Escola Superior de Biotecnologia, Rua de Diogo Botelho, 1327, 4169-005 Porto, Portugal

9 [c] Université de Lorraine, CNRS, LCPME, F-54000, Nancy, France

10 [d] Technische Universität Dresden, Institute of Hydrobiology, Dresden, Zellescher Weg 40, Germany

11 [e] Fluence Corporation, Caesarea, Israel

12 [*] Equal contribution

13

14

15

16

17

18

19

20

21

22

23

24

25

26

Abstract

Antibiotic resistant bacteria and antibiotic resistance gene (ARG) loads dissipate through sewage treatment plants to receiving aquatic environments, but the mechanisms that mitigate the spread of these ARGs are not well understood due to the complexity of full-scale systems and the difficulty of source tracking in downstream environments. To overcome this problem, we targeted a controlled experimental system comprising of a semi-commercial membrane-aerated bioreactor (MABR), whose effluents fed a 4500 L polypropylene basin that mimicked effluent stabilization reservoirs and receiving aquatic ecosystems. We analyzed a large set of physicochemical measurements, concomitant to cultivation of total and cefotaxime-resistant *Escherichia coli*, microbiome analyses and qPCR/ddPCR quantification of selected ARGs and mobile genetic elements (MGE). The MABR removed most of the sewage-derived organic carbon and nitrogen, and simultaneously *E. coli*, and ARG and MGE levels dropped by approximately 1.5- and 1.0-log unit ml^{-1}, respectively. Similar levels of *E. coli*, ARGs and MGEs were removed in the reservoir, but interestingly, unlike the MABR, the relative abundance (normalized to 16S rRNA-gene inferred total bacterial abundance) of these genes also decreased. Microbiome analyses revealed more significant shifts in bacterial and eukaryotic community composition in the reservoir relative to the MABR. Collectively, we conclude that the removal of ARGs in the MABR is mainly a consequence of treatment-facilitated biomass removal, whereas in the stabilization reservoir, mitigation is linked to natural attenuation associated with ecosystem functioning, which includes abiotic parameters, and the development of native microbiomes that prevent establishment of wastewater-derived bacteria and associated ARGs.

Keywords: Wastewater treatment, ecological barriers, community shifts, antibiotic resistant bacteria, antibiotic resistance genes, mobile genetic elements, microbiome, qPCR, ddPCR

Introduction

Raw sewage is a mirror of the gut microbiota of the served population [1], and is consequently a source of fecal-derived antibiotic resistant bacteria (ARB) and resistance genes (ARGs), whose abundance and diversity vary as a function of geography and socioeconomic conditions [2, 3]. Although ARGs are minor components of the sewage metagenome (0.03%), the sewage resistome constitutes a vast array of genetic determinants that confer resistance to the entire spectrum of antibiotic classes, including ARGs associated with emerging clinical threats [2, 4]. Conventional wastewater treatment processes based on activated sludge generally remove 1-3 log-units ml^{-1} (per volume) of total and antibiotic resistant fecal bacteria [5] and associated ARGs [6], and this removal can be augmented by disinfection [6], and membrane-based processes [7]. Nonetheless, wastewater treatment plant (WWTP) effluents frequently contain substantial ARB and ARG loads [8-13]. Discharge of these determinants to receiving aquatic ecosystems or irrigated soils can result in their dissemination through the water cycle and/or the food chain, potentially expanding the global scope of antibiotic resistance [14-16].

Fecal bacterial indicators that are routinely targeted for water quality assessment provide no insights regarding antibiotic resistance. This can be overcome by monitoring fecal bacterial indicators resistant to next-generation antibiotics concomitant to total counts [5], as proposed in a recent review [18]. Source tracking of ARGs using quantitative PCR-based methods provide a rapid and accurate means of quantification that sheds light on antibiotic resistance levels in WWTPs and receiving environments, but there are close to 3000 documented antibiotic resistance determinants [19], and currently there are no established ARG standards for assessing water quality. Within an epidemiological context, ARGs are only interesting to monitor if they can be horizontally transferred to other bacteria and/or they are associated with pathogens. With this respect, Zhang et al. proposed ranking ARGs according to the associated risk level for human health, where rank I refers to ARGs that are associated with mobile genetic elements (MGEs) and are present in ESKAPE pathogens [21]. The limitations of both cultivation-based and culture-independent molecular analyses underline the fact that combining the two is imperative for holistic understanding of antibiotic resistance in WWTP effluents and downstream environments.

In warm, water depleted countries (*i.e.* Israel) that reuse wastewater for irrigation, effluent storage (or stabilization) reservoirs with capacities reaching 5 million m^3, enable modulating between relatively constant sewage production and generally irregular (seasonal) demand for irrigation water. These hypertrophic aquatic systems that operate under non-steady-state conditions [24],have the capacity to improve effluent quality (*i.e.* reduce loads of fecal pathogen indicators and recalcitrant organic compounds), with sufficient retention times [25]. Various studies have investigated the fate of WWTP effluent-derived ARB and ARG in receiving aquatic ecosystems [13, 21-23]. While certain studies indicate that ARGs can

89 persist in receiving water and sediment (22), others suggest that they are either diluted or actively removed
90 (13). These studies highlight the fact that mitigation of sewage derived ARB and ARGs in these receiving
91 aquatic ecosystems is associated with ecological interactions (23), but the scope and nature of these
92 interactions are still not well understood due to environmental complexity and difficulty of source tracking
93 (21).

94   The goal of this study was to elucidate the scope, dynamics and potential mechanisms responsible for
95 ARB and ARG removal in a large-scale pilot system containing a semi-commercial scale membrane
96 bioreactor treating municipal sewage, specifically focusing on a large (4500 L) pilot stabilization reservoir.
97 We applied a holistic analytical pipeline that measured physicochemical analyses, cultivation of total and
98 antibiotic resistant fecal coliforms, microbiome (bacterial and eukaryotic) analysis and quantification of
99 potentially hazardous ARGs and associated MGEs markers (qPCR and ddPCR) along the sewage-effluent-
100 reservoir trajectory. The closed nature of the system and the coupling of isolation, culture-independent ARG
101 quantification and analysis of microbial community composition provided important insights into the
102 mechanisms potentially responsible for mitigation antibiotic resistance in WWTPs and receiving reservoirs,
103 which may portray other aquatic ecosystems.

Materials and Methods

Description of experimental system

106   An experimental wastewater treatment beta-site (**Figure. 1**), situated within the Maayn Zvi municipal
107 wastewater treatment plant (32.59684, 34.92975) in Israel, was operated between July and December 2020.
108 The system consisted of an Aspiral L3 ([www.fluencecorp.com/wp-content/uploads/2018/05/Aspiral-](http://www.fluencecorp.com/wp-content/uploads/2018/05/Aspiral-Product-Brochure.pdf)
109 [Product-Brochure.pdf](http://www.fluencecorp.com/wp-content/uploads/2018/05/Aspiral-Product-Brochure.pdf)) Membrane Aerated Biofilm Reactor (MABR) connected to a cylindrical
110 polypropylene reservoir (4500 L working volume), aimed to mimic operational reservoirs commonly used
111 for effluent storage prior to irrigation. The passive aeration by diffusion of oxygen through MABR
112 membranes supports an aerobic nitrifying biofilm that develops on their surface, while suspended solids are
113 held in the mixed liquor, enabling simultaneous nitrification and denitrification. To date, approximately 300
114 commercial decentralized MABR units have been installed at various sites in Asia, Africa and North
115 America. The feed flow rate of primary effluent to the MABR was approximately 5 m^3/h with slight
116 variations due to occasional equipment failures (*i.e.* clogged feed pump, ruptured diffuser), power failures (4
117 overall) and excess sludge removal, which reduced the desired effluent quality. Mixing frequency and
118 duration, Return Activated Sludge (RAS), Sludge wasting (WAS) and aeration regimes were modulated to
119 maintain bioreactor performance. Reservoir retention time was initially 21 days (from system initiation to
120 October 14th, 2020), after which it was reduced to 10 days (October 14th, 2020 to November4th, 2020), and

121 later on 5 days (November 4th, 2020 to November 25th, 2020) in order to evaluate the potential impact on the

122 capacity of the reservoir to remove fecal bacteria and ARGs.
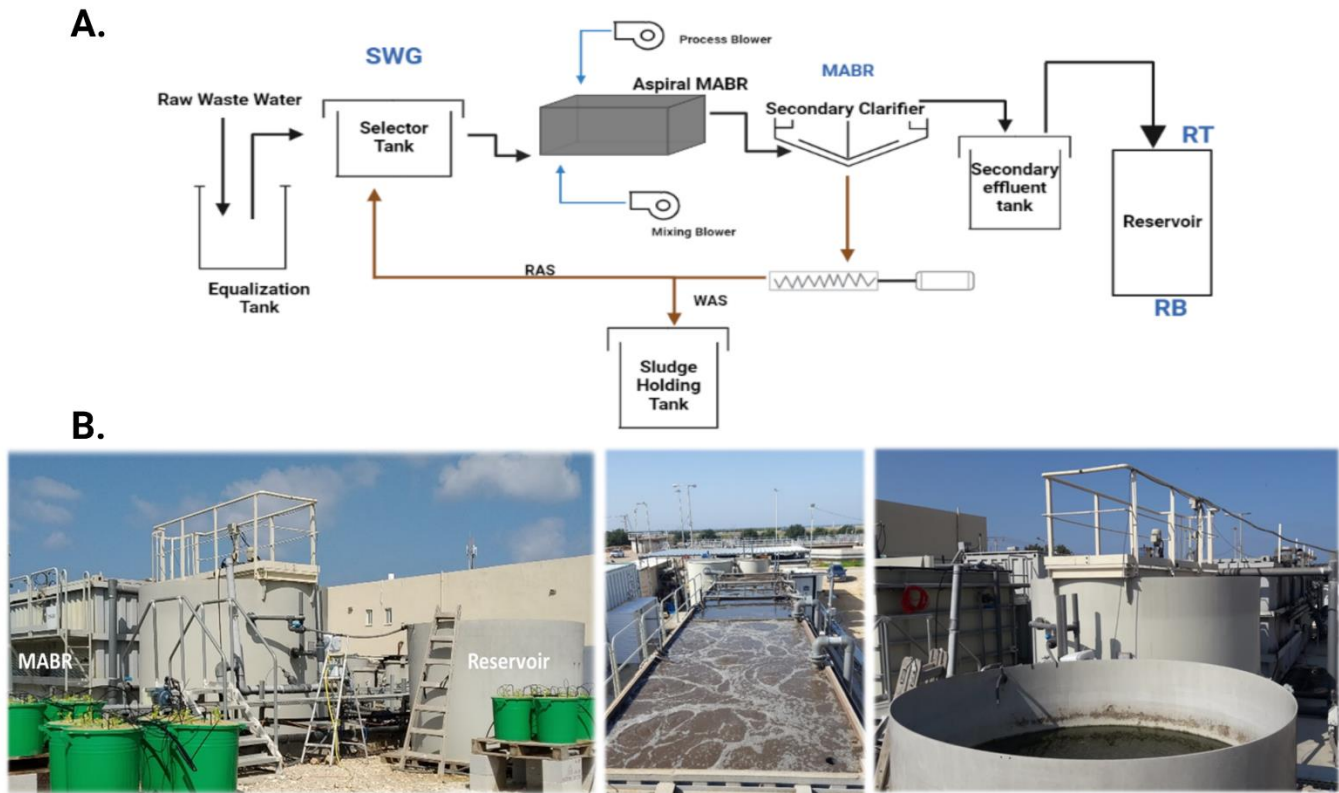
123

124 **Figure 1. Overview of the experimental beta-site.** A.) Schematic diagram of the raw sewage-Membrane

125 Aerated Biofilm Reactor (MABR)-reservoir continuum at the beta-site. Sampling points SWG (raw

126 Sewage), MABR (membrane aerated bioreactor) and RES (reservoir) with RT (reservoir top): Sampling

127 faucet situated at the top 10 cm of the reservoir; RB (reservoir bottom): Sampling faucet situated at the

128 bottom 10 cm of the reservoir. B.) Profile (Left) and aerial photos of the MABR (middle) and reservoir

129 (Right) at the beta-site.

130

131   Samples for physicochemical, bacterial and molecular analyses (**Table S1**) were taken from faucets

132 situated at different points along the sewage-MABR-reservoir trajectory (**Figure. 1**). Faucets were opened

133 for 30s and sampling vessels were washed 3 times before sampling to remove residual water in the pipes.

134 Water samples for bacterial enumeration and community DNA extraction were either immediately filtered

135 on site or transferred on ice to the lab at the Volcani Institute and filtered within 3 h. Samples for

physicochemical analyses and bacterial quantification were taken from July 22, 2020; whereas samples for microbiome and quantitative PCR analyses were taken from August 19, 2020.

Physical and Chemical analyses

Temperature, oxygen, pH and conductivity were measured using a HQ40D model digital two channel multi meter (HACH, CO, USA) using specific electrodes for each parameter, and turbidity was measured with a 2100Q Portable turbidimeter (HACH, CO, USA). Total organic carbon (TOC) was determined by dry combustion with a Flashea™ 1112 NC elemental analyzer (Thermo Fisher Scientific, Hanau, Germany). Ammonia, nitrite, nitrate, phosphorus and sulfate were measured colorimetrically with a Quickchem 8000 Autoanalyzer (Lachat Instruments, Milwaukee, WI) using standard protocols provided by the manufacturer.

Microbial quantification, isolation and characterization

Cultivation-based analysis was applied to enumerate total and cefotaxime-resistant coliform and *Escherichia coli* in the raw sewage, MABR effluent and reservoir, using a modified version of the standard membrane filtration method (ISO 9308-1). Briefly, ten-fold serial dilutions (10^{-2} to 10^{-5}, and 10^{0} to 10^{-4} for total and cefotaxime resistant coliforms, respectively) of the collected raw sewage and effluent samples were prepared in sterile saline solution (0.85% (w/v) NaCl) and 1 ml of diluted sample was filtered in triplicates through a 0.45 µm nitrocellulose grid membrane filter using a vacuum filtration system. Subsequently, filters were placed (grid facing upwards) on CCA (Coliform Agar acc. to ISO 9308-1 Chromocult®) culture media plates with or without cefotaxime (4 mg/L), which is above CLSI and EUCAST clinical breakpoints for *E. coli* (26) and plates were incubated at 37 °C overnight. Coliform and *E. coli* colonies on the CCA media were enumerated based on the color classification defined by the supplier.

To validate presumptive CCA colorimetric identifications, 108 randomly-selected colonies from raw sewage, MABR and the reservoir were classified on a microflex LT MALDI-TOF MS system (Bruker Daltonics GmbH, Bremen, Germany) using the Flex Control v3.4 Biotyper automation software as previously described (27). Results supported the manufacturer's colorimetric taxonomic characterizations, as: 55 blue colonies were identified as *E. coli* or *Shigella* and 53 red colonies were identified as *Klebsiella* spp. and *Enterobacter* spp.

DNA extraction, storage, and shipment

For DNA extraction, 10 to 100 ml of the freshly collected samples were filtered through 0.22 µm polycarbonate membranes using a filtration unit and then stored at -80 °C prior to extraction. Sampling dates and specific volumes filtered for each sample are shown in **Table S2**. DNA was extracted from these

166   membranes using the DNeasy PowerWater kit (cat# 14900-100-NF, Qiagen, USA), using the protocols

167   provided by the manufacturer. Purified DNA was divided into four aliquots and stored at -80 °C, until

168   shipping. Composite (top and bottom) reservoir samples were prepared by mixing equal volumes of DNA,

169   after top and bottom physicochemical parameters were found to be very similar to each other. Samples for

170   bacterial community analysis and qPCR quantification of ARGs were shipped to Universidade Católica

171   Portuguesa in Porto, Portugal; samples for ddPCR quantification of ARGs and MGEs were shipped to

172   Université de Lorraine, Nancy, France; and samples for eukaryotic community analysis were shipped to

173   Technische Universität Dresden, Germany. All samples were shipped on dry ice by 2-day express delivery

174   and stored at -80 °C upon arrival.

Quantification of 16S rRNA gene, Mobile Genetic Elements & Antibiotic Resistance Genes

176   Digital droplet PCR (ddPCR) and quantitative PCR (qPCR) were applied to quantify the bacterial

177   16S rRNA gene, the *Escherichia coli* indicator gene *uidA* and the CrAssphage fecal contamination indicator,

178   as well as five ARGs (*sul1*, *ermF*, *bla*$_{VIM-2}$, *bla*$_{KPC}$, *bla*$_{CTX-M-1}$) and four MGE families (class 1 integrons,

179   Tn*916*/Tn*1545* ICE family, SXT ICE family, IncP plasmid family). The above-mentioned genes were all

180   analyzed on the samples from the following dates: 19th and 25th of August, 15th of September, 24th of

181   November, 1st and 15th of December 2020. The ddPCR was conducted on a One-Step QX200 system (Biorad

182   Hercules, CA, USA) using the Evagreen or Taqman technologies. The qPCR was performed on a

183   StepOnePlus™ machine (Applied Biosystems, Life Technologies, Carlsbad, CA, USA) using TaqMan

184   technology (**Table S3**). Sample dilution were adjusted to avoid saturation with 100% of positive droplets

185   (for 16S rRNA genes for instance), and the absolute number of target copies was calculated from the

186   proportion of positive partitions and statistically corrected with a Poisson distribution. Primers, mix reactions

187   and amplification conditions for ddPCR and qPCR are described in **Table S3**. For ddPCR, the QX

188   Manager™ software (version 1.7.4, BioRad) was used to assign positive/negative droplets after adjusting the

189   thresholds manually, and to convert counts into copies/µL. Negative controls (DNA- and RNA-free water),

190   and a positive control (artificial target DNA) were used in the first ddPCR assay, to confirm the proper

191   position of the positive/negative droplets. Negative controls and a calibration curve were run with each qPCR

192   determination. We initially compared qPCR and ddPCR quantifications of 16S rRNA and *ermF* genes using

193   identical sets of DNA to determine the relation between the two approaches (**Figure S1**).

194   The rationale for choosing the targeted genes is as follows. The beta-glucuronidase encoding *uidA*

195   gene was chosen because it is frequently used to source track *E. coli* (the most common fecal bacterial

196   indicator) in aquatic ecosystems, and the CrAssphage bacteriophage was selected because it is highly

197   abundant in the human gut. The ARGs were targeted based on expected abundance and ubiquity and different

198   risk levels according to Zhang *et al.* , included the widespread *sul1* gene (rank IV), the human-enriched *ermF*

199 gene (rank III/IV), and three ARGs of concern to public health, *bla*$_{CTX-M-1}$ (rank III), *bla*$_{VIM-2}$ (rank I/III), and

200 *bla*$_{KPC-2}$ (rank I). Regarding the rationale for MGE selection, Tn*916*/Tn*1545* ICE family is abundant in

201 *Bacillota*, the SXT/R391 ICE family is predominant in *Gammaproteobacteria*, IncP-1 conjugative plasmids

202 are profuse in *Pseudomonadota*, and Class 1 integrons are broadly found in Gram-negative bacteria.

Microbial community analyses

204   Prokaryotic communities were analyzed by targeting the V3-V4 region of the 16S rRNA gene, using

205 the primers 341F and 806R (**Table S3**). Amplicons were sequenced using an Illumina paired-end platform

206 to generate 250 bp paired-end raw reads that were merged with FLASH (V1.2.7) and quality filtered using

207 QIIME software (V1.7.0). The chimeric sequences were removed and the reads with good quality were

208 assigned to operational taxonomic units (OTUs; ≥97% sequence identity). OTUs annotation was performed

209 against the SSUrRNA SILVA v.138 Database (http://www.arb-silva.de/) (29). The weighted UniFrac

210 distance matrix was used to generate a Principal Coordinate Analysis (PCoA) and a features table used for

211 sample comparison and statistical analysis performed with STAMP software (v2.1.3).

212   Eukaryotic communities were analyzed by targeting the 18S rRNA gene using the universal primers

213 1391f and EukBr (30) (**Table S3**) that target the V9 variable region. PCR products with proper size were

214 selected following validation by 2% agarose gel electrophoresis. Equimolar amounts of PCR products from

215 each sample were pooled, end-repaired, A-tailed and further ligated with Illumina adapters. Libraries were

216 sequenced at Novogene Co. (Cambridge, UK) using the Illumina MiSeq platform generating 250 bp paired-

217 end raw reads, which were assigned to samples based on their unique barcodes and truncated by cutting off

218 the   barcode   and   primer   sequences.   Subsequently,   FLASH   (28)   (v1.2.11,

219 http://ccb.jhu.edu/software/FLASH/) was applied to merge reads, and fastp for quality control of raw tags,

220 to obtain high-quality clean tags. Vsearch software (32) was used to blast clean tags against the database, to

221 detect and remove chimeric sequences. The deblur module in QIIME2 (33) was used to denoise, and

222 sequences with less than 5 reads were filtered out to obtain the final ASVs (Amplicon Sequence Variables)

223 and feature table. Finally, the Classify-sklearn module in QIIME2 software was used to compare ASVs with

224 the SILVA Database (http://www.arb-silva.de/)(29), and to obtain the species annotation of each ASV. In

225 tandem, the weighted UniFrac distance for PCoA analysis was calculated in QIIME2.

226   The 16S and 18S rRNA sequences were uploaded to the NCBI-SRA archive under Bioproject number

227 PRJNA805207.

Statistical analyses

229   One-way ANOVA followed by an LSD post-hoc test was applied to evaluate statistical significance
230   between the raw sewage, MABR and reservoir for each of the measured parameters, and one-way ANOVA
231   followed by a Tukey-Kramer post-hoc test was applied to evaluate temporal variance. For all analyses,
232   differences were considered significant when p-values were below 0.05.

233   Potential relationships between species-level microbial community composition and structure,
234   ARG&MGE markers, and environmental and physicochemical variables were assessed using Redundancy
235   Analysis with Canoco 5.01 software (34). The relationship between species and environmental variables was
236   assessed based on 1000 Monte Carlo permutations, followed by forward selection with the criterion of $p<0.01$
237   of significance.

238   IBM SPSS Statistics version 28 was used to statistically analyze the alpha diversity of the most
239   abundant prokaryotic (>5%) and eukaryotic microbiomes (>1%) and for comparing the qPCR and ddPCR
240   analyses (UCP and LCPME labs, respectively) of 16S rRNA and *ermF* genes. For alpha diversity, ANOVA
241   was applied with Tukey as post-hoc test with a significance level of $p<0.01$. For the comparison between
242   laboratory results, a Friedman test was performed (with significance level of $p<0.01$) because the data did
243   not follow a normal distribution. Statistical calculations for gene abundance and microbial community
244   analyses are shown in **Tables S5-S8**.

Results

Physicochemical fluctuations along the sewage-MABR-stabilization reservoir trajectory

247   We evaluated physicochemical parameters along the sewage-MABR-stabilization reservoir trajectory
248   between July and December 2020, at 17 time points. Water temperatures ranged from 35 to 17 $^{\circ}$C. In the
249   November and December profiles, reservoir temperatures were approximately 5 $^{\circ}$C lower than the raw
250   sewage (**Figure. 2A**), indicating that they are more strongly impacted by ambient temperatures. The pH
251   (**Figure. 2B**) and dissolved oxygen levels (**Figure. 2C**) were relatively stable in raw sewage and the MABR
252   (except for 22nd July and 8th September 2020 where oxygen in the MABR was low due to system
253   malfunction), but varied more in the stabilization reservoir, seemingly due to photosynthetic activity.
254   Turbidity (**Figure. S2A**) was almost completely alleviated in the MABR (with the exception of September
255   1st and 8th, 2020 when malfunctions occurred), correlating to significant reduction in total organic carbon
256   (**Figure. 2D**). Likewise, over 80% of total nitrogen was removed in the MABR (**Figure. 2E**), corresponding
257   to the removal of most of the ammonia (**Figure. 2F**). Mass balance of all the analyzed species indicated that
258   most of the carbon and nitrogen in the system was either gasified (to CO_2, N_2 or N_2O) or removed as settled
259   sludge biomass, considering the fact that N-nitrate (**Figure. 2H**) and N-nitrite (**Figure. 2G**) concentrations
260   in the MABR effluent were 1-2 orders of magnitude lower than the influent N-ammonia concentration.

261 Phosphate levels (**Figure. S2B**) significantly dropped between raw sewage and MABR suggesting

262 accumulation of polyphosphate in sludge biomass, and sulfate (**Figure. S2C**) increased between raw sewage

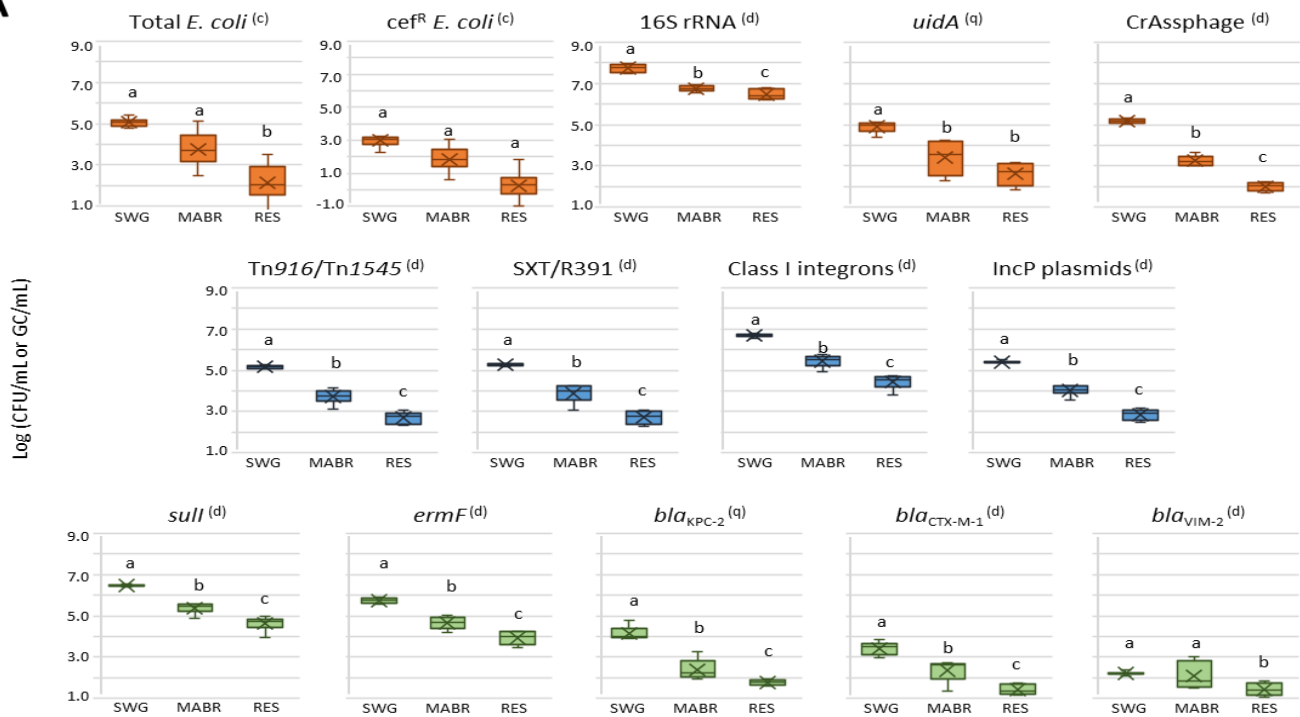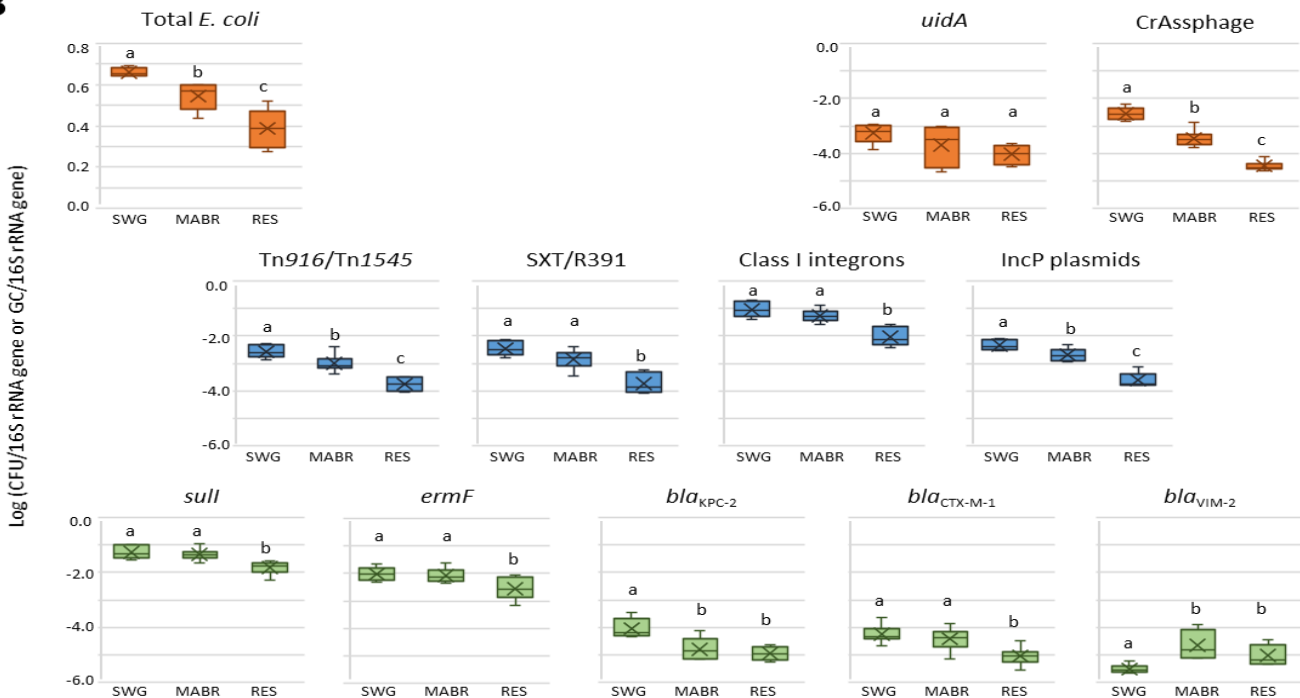263 and MABR, implying oxidation of reduced sulfur compounds such as H_2S.
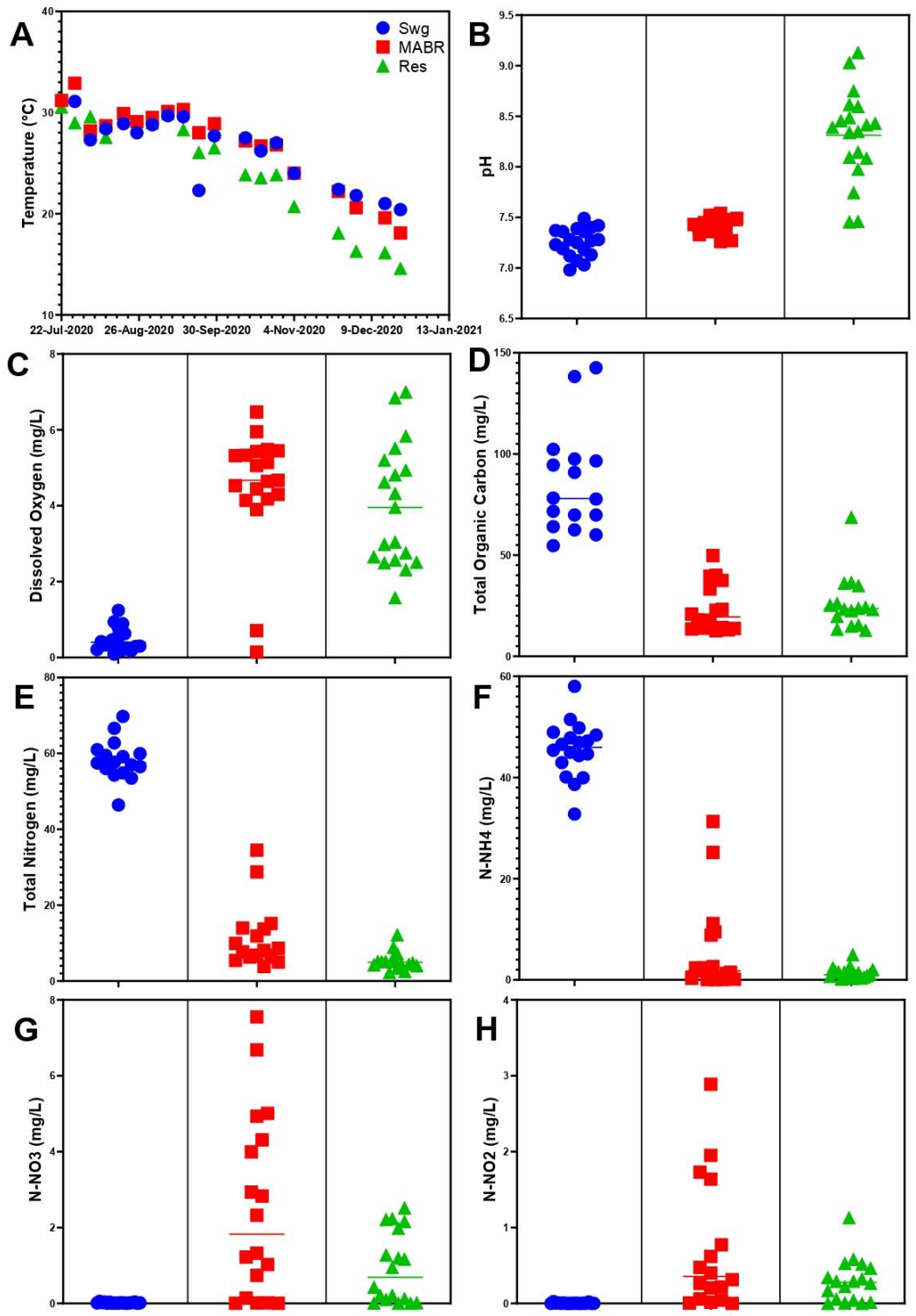
264 **Figure 2. Physicochemical analyses** in the raw sewage (blue circles), MABR (red boxes) and reservoir

265 (green triangles). Temperature (A); pH (B); dissolved oxygen (C); total organic carbon (D). Total nitrogen

266 (E); ammonia (F); nitrate (G); nitrite (H).

267

Fecal coliform dynamics along the sewage-MABR-stabilization reservoir trajectory

268

269   We evaluated abundance of total and cefotaxime-resistant *E. coli* (**Figure 3A**) and fecal coliforms
270   (**Figure S3**) in the targeted compartments. On average, the abundance of these fecal bacterial indicators
271   decreased by approximately 1.5 log units ml^{-1} in both the MABR and stabilization reservoir, although
272   fluctuations in removal capacity in both modules were observed at different time points (**Figure S4**).
273   However, normalizing to the 16S rRNA gene levels measured by quantitative PCR analyses (**Figure 3B**),
274   revealed that the abundance of *E. coli* relative to the total bacterial community decreased more in the
275   stabilization reservoir than in the MABR. *E. coli* values measured in the raw sewage and MABR were similar
276   to levels of the *E. coli* marker gene *uid*A (see below), supporting the culture-based analyses. In contrast, in
277   the reservoir *uid*A levels were slightly higher than cultivated *E. coli* levels, suggesting the presence of free
278   DNA or non-viable bacteria.

ARG&MGE dynamics along the sewage-MABR-stabilization reservoir trajectory

279

280   The abundance of the nine targeted ARG&MGE markers was monitored by qPCR/ddPCR in the raw
281   sewage, MABR and stabilization reservoir on six sampling dates (August 19th and 25th; September 15th;
282   November 24th; and December 1st and 15th, 2020; **Figure. 3A**). In parallel, 16S rRNA, *uidA* and CrAssphage
283   genes were monitored to estimate total bacterial, *E. coli* and *Bacteroides* phages, respectively. The low
284   standard deviations observed for most of the targeted genes indicate that the abundance of these markers is
285   relatively steady over time in each module. On average, bacterial loads (estimated by 16S rRNA gene
286   abundance) dropped from 8.2 log-units ml^{-1} in sewage to 7.1 log-units ml^{-1} after MABR treatment, and to 6.7
287   log-units in the stabilization reservoir. Apart from *bla*$_{VIM-2}$, all the gene markers followed the same trend
288   with an approximate 2-order of magnitude reduction across the trajectory (**Figure. 3A** and **Figure. S5**).
289   However, excluding *bla*$_{VIM-2}$, the reduction in normalized ARG&MGE abundance (**Figure. 3B**) was higher
290   in the stabilization reservoir than in the MABR, similar to the trend observed for *E. coli* described above.
291   Most notably were SXT/R391, class 1 integrons, incP plasmids, *sul*1, *erm*F and *bla*$_{CTX-M-1}$, whose reduction
292   in relative abundance was only significant (p-value < 0.05) in the stabilization reservoir.

Figure 3. (A) Absolute and (B) relative abundances of total and cefotaxime-resistant *E. coli* and of 12 ARGs/MGEs markers. . Each data point represents aggregated data collected from six different sampling times and four biological replicates. One-Way ANOVA Test followed by pairwise two sample t-test highlights significant differences. Colors represented different groups: MGE (blue), ARG (green) and bacterial (orange) markers and indicators (CrAssphage with CPQ_056 gene). The boxes indicates the range between the first and third quartile. The top and bottom whiskers of the boxes represent maximum and the minimum values, respectively. The median line divides the box into interquartile range and the cross

represents the mean. Each box represent the spread of time point averages (four biological replicates per time point).

Microbial diversity along the sewage-WWTP-stabilization reservoir trajectory

Rarefaction curves (**Figure. S6**) and diversity indexes of bacterial communities varied between samples (**Table S4**) and sampling times. Average Shannon and Phylogenetic Diversity indices were higher in the raw sewage and MABR than in the reservoir, but the variance in the diversity indices was substantially higher in the stabilization reservoir, highlighting the dynamic nature of this ecosystem.

PCoA analyses revealed a strong distinction between raw sewage, MABR and reservoir bacterial communities (Figure 4,right). Raw sewage bacterial communities appeared to be highly stable for the
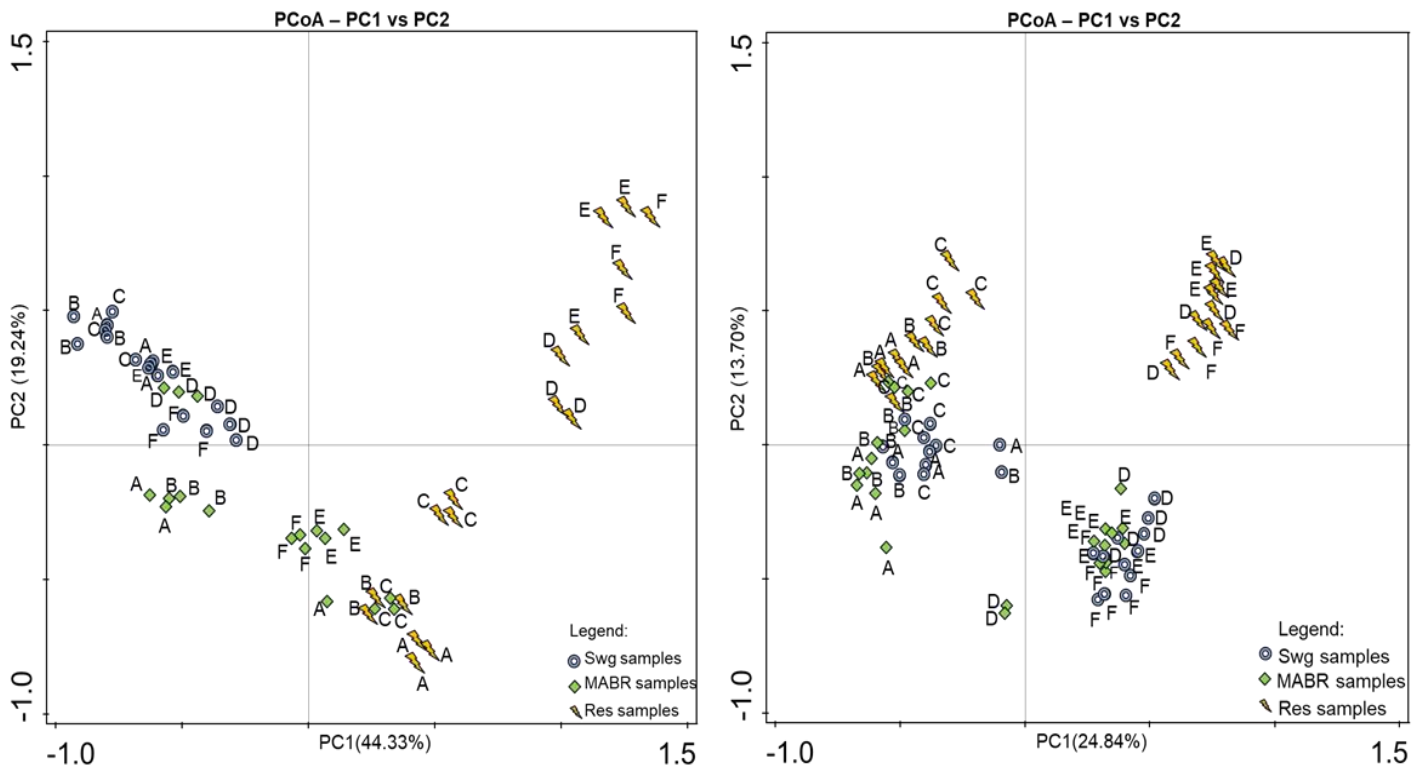
duration (August-December, 2020) of the analysis. In contrast, the composition of MABR bacterial communities fluctuated more, but these shifts were not completely seasonally dependent. The bacterial communities in the stabilization reservoir displayed the strongest fluctuations, principally dictated by seasonality. In contrast, the eukaryotic community dynamics (Figure 4left) were substantially different from the bacteria, and clustered into three primary clades. The first clade encompassed all of the samples from all three modules of the August and September profiles. The second clade contained raw sewage and MABR samples from the November and December samples, and the third clade contained all of the reservoir samples from November and December.

318 **Figure 4**. **Bacterial and Eukarya community composition, structure and diversity**. Prokaryotic (Left)
319 and Eukaryotic (right) diversity in raw sewage (Swg), MABR and Reservoir (Res) samples. Sampling dates
320 A – August 19th, B – August 25th, C – September 15th, D – November 24th, E – December 1st and F –
321 December 15th.

322

323 *Microbial community composition along the sewage-WWTP-stabilization reservoir trajectory*

324 The phylum level evaluation of raw sewage, MABR and reservoir samples revealed distinct bacterial
325 community profiles (**Figure. S7A**). The reservoir samples collected in November and December were richer
326 in *Cyanobacteria* than in the previous sampling times. Family-level analysis suggested that *Cyanobacteria*
327 were, indeed, predominantly chloroplasts (**Figure. S5A**), corresponding to eukaryotic algae also predominant
328 in these microbial community profiles. Members of the phyla *Pseudomonadota* (31.9% SWG, 37.7%
329 MABR, 34.1% RES), *Bacteroidota* (11.0% SWG, 14.0% MABR, 15.4% RES) and *Actinobacteriota* (6.7%
330 SWG, 10.9% MABR, 11.9% RES) were among the most represented in all samples, with the relative
331 abundance of *Bacillota* and *Campylobacteriota* sharply decreasing from raw sewage to the reservoir (13.1%
332 to 4.7% and 26.9% to 3.6%, respectively). In contrast, the relative abundance of other groups increased in
333 the reservoir along the different sampling times. Most notably *Cyanobacteria* (ranging from 2.6% to 43.7%,
334 in December), *Pseudomonadota* (ranging from 27.6% to 41.3 in August) and *Verrucomicrobiota* (ranging
335 from 0.4% to 11.9 in September), in a pattern that was sampling-date-dependent. Analysis of the eukaryotic
336 community (**Figure. 5B**; **Figure. S7B**) revealed that for the duration of the analysis, the MABR was
337 dominated by the bacterivorous protists *Ciliophora* (13.4–25.8% rel. abundance), with the exception of a
338 brief period when *Euglenazoa* (up to 32.9 ± 9.1% at 25th August 2020) and *Ochrophyta* (up to 62.8 ± 9.3%
339 at 15th September 2020) became dominant, corresponding to the above described MABR malfunction.
340 Initially, the reservoir was dominated by *Ciliophora* (38.8 ± 2.0%), the dominant eukaryote in the MABR,
341 and by *Proteoalveolata* (22.5 ± 2.3%), which was less abundant in the MABR. However, the relative
342 abundance of both groups significantly decreased with time (p=0.02; n=24; non-parametric test for
343 association based on Spearman's rho), with *Proteoalveolata* dropping below detection levels, and the relative
344 abundance of *Ciliophora* dropping to 5.2 ± 0.6 %. Conversely, the relative abundance of *Chlorophyta* (green
345 algae) significantly increased over time (p<0.001; n=24; ANOVA) and became the dominant phyla from
346 November onward, accounting for more than 75% of the relative abundance of eukaryotes in the reservoir.
347 This taxa strongly correlated to the increase in relative abundance of chloroplasts described observed in the
348 bacterial community analysis. This increase in *Chlorophyta* abundance was identified as the primary driver
349 of the observed eukaryotic community composition shift (p<0.01; n=24; AMOVA (Analysis of MOlecular

VAriance) relative to the three early profiles where blooms of this group of green algae were not observed
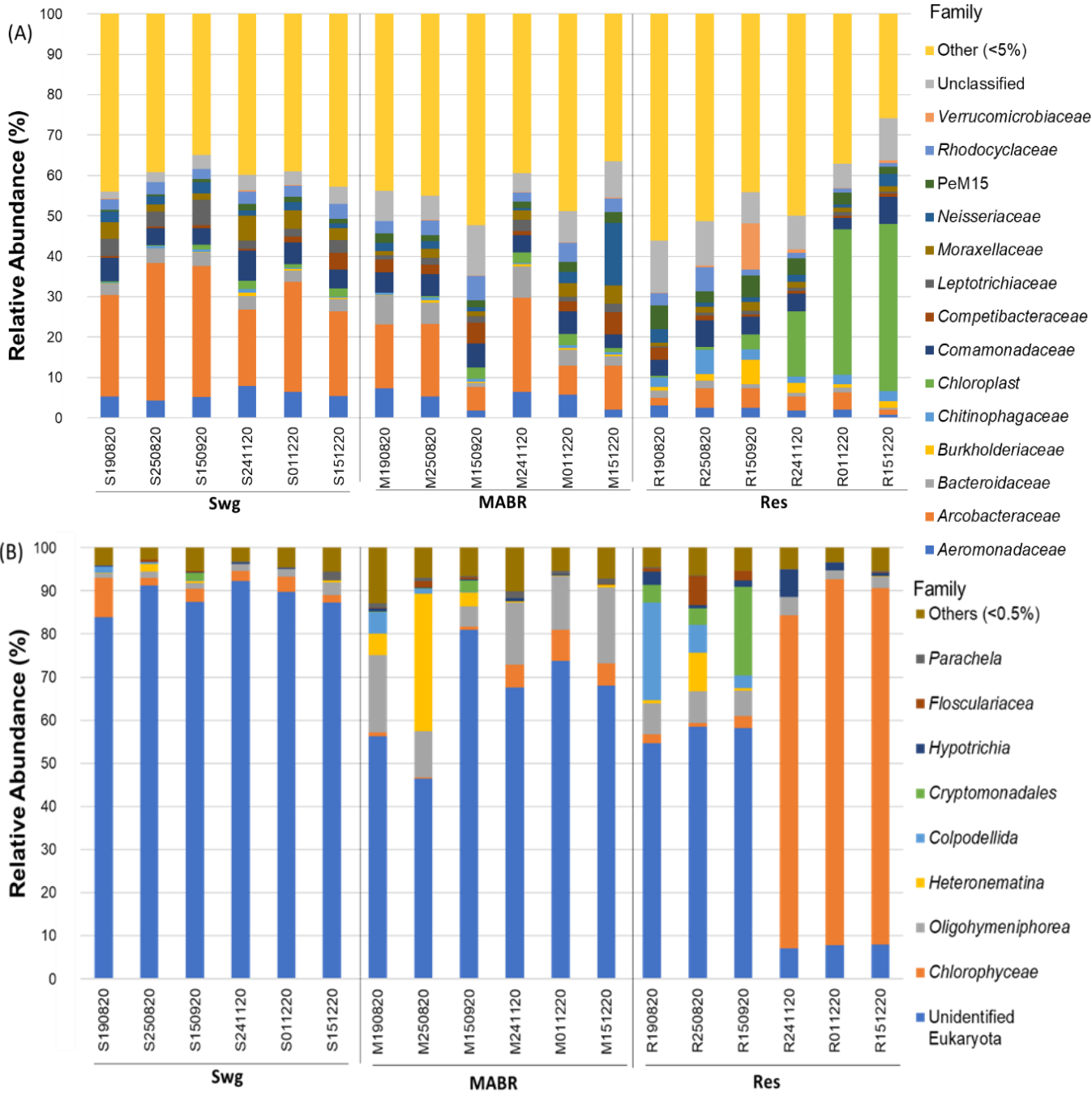
in the reservoir.

Figure 5. Microbial community composition. Dominant bacterial (A) and eukaryotic (B) families based on 16S rRNA (V3-V4) and 18S rRNA (V9) gene amplicons, respectively, in the raw sewage (Swg), MABR and reservoir (Res) samples. Only families with relative abundance of >5% and >1% for the bacteria and eukarya, respectively are shown. MGEs and *uidA* gene in function of the prokaryotic and eukaryotic community phyla members with relative abundance >5% and >1%, respectively, and summed as others (E,

358   eukaryote or P, prokaryote) for lower values. Additional information and statistical analyses are provided in
359   **Table S9**. (C) and (D) - Redundancy analysis (RDA) of the variation ARGs, MGEs and 16S rRNA genes in
360   M and R samples in function of prokaryotic community. The test variables (ARGs, MGEs and uidA) are
361   represented in black and the explanatory (prokaryotes) in blue. The explanatory variables were associated
362   with 78.7% of the observed variation among the test variables.

363

364   We applied the STAMP software, to identify bacterial and eukaryote classes and families that are
365   differentially abundant in the MABR *vs.* the stabilization reservoir (**Figure 6**). *Arcobacteraceae*,
366   *Bacteroidaceae*, *Aeromonadaceae*, *Competibacteraceae*, *Rhodocyclaceae* and *Leptotrichiaceae* were the
367   primary MABR-enriched bacterial families, and the ciliate *Oligohymenophorea* was the primary eukaryotic
368   family. In contrast, in the stabilization reservoir, *Chitinophagaceae*, *Burkholderiaceae,* Ca. Aquilina PeM15
369   and the cyanobacteria *Microcystaceae* were the dominant bacteria and the algae *Chlorophyceae*, were the
370   dominant eukaryotes. Collectively, all of the families that were differentially abundant in the MABR are well
371   established in wastewater treatment systems and specifically in activated sludge, whereas those that were
372   more abundant in the stabilization reservoir are more abundant in freshwater ecosystems.
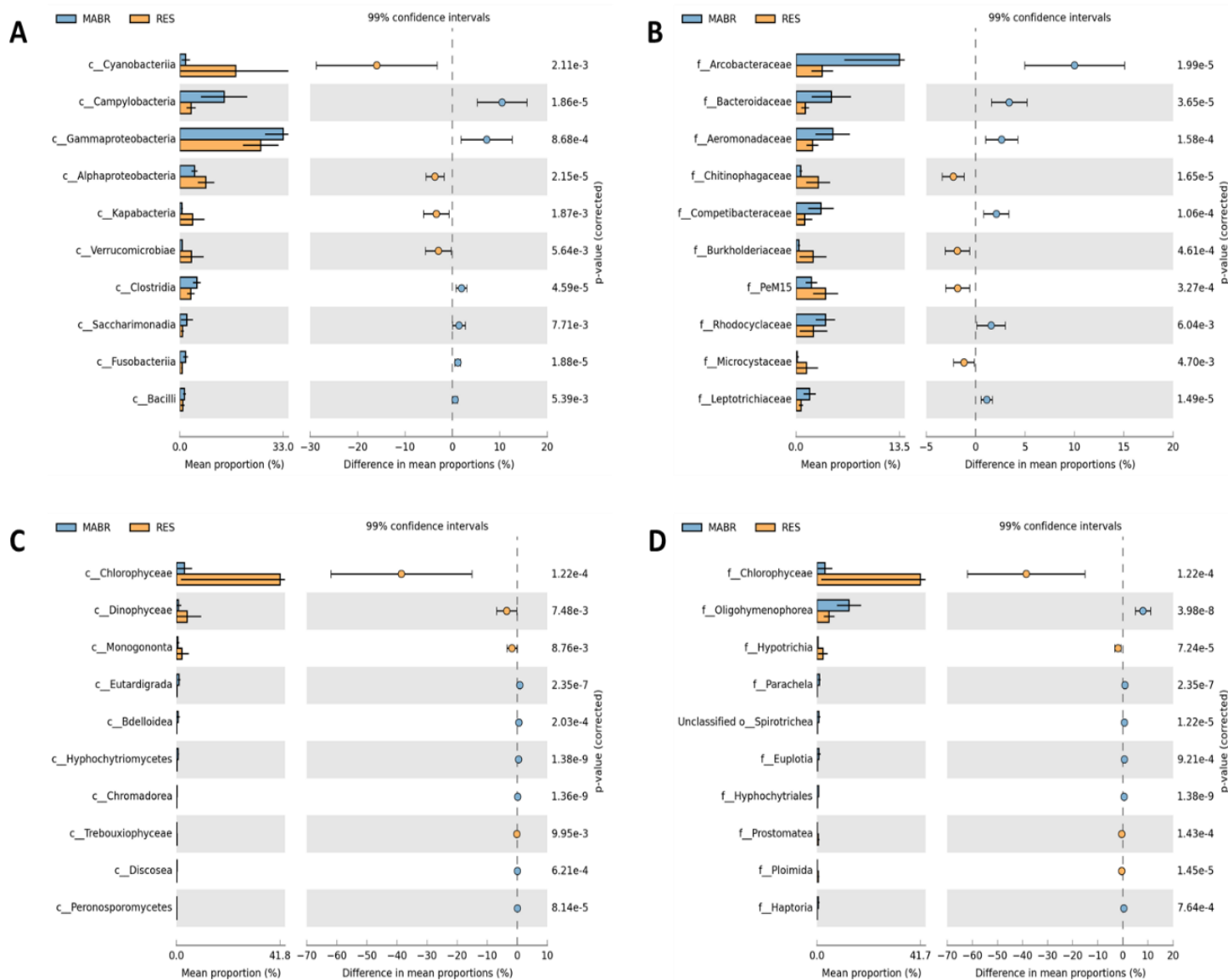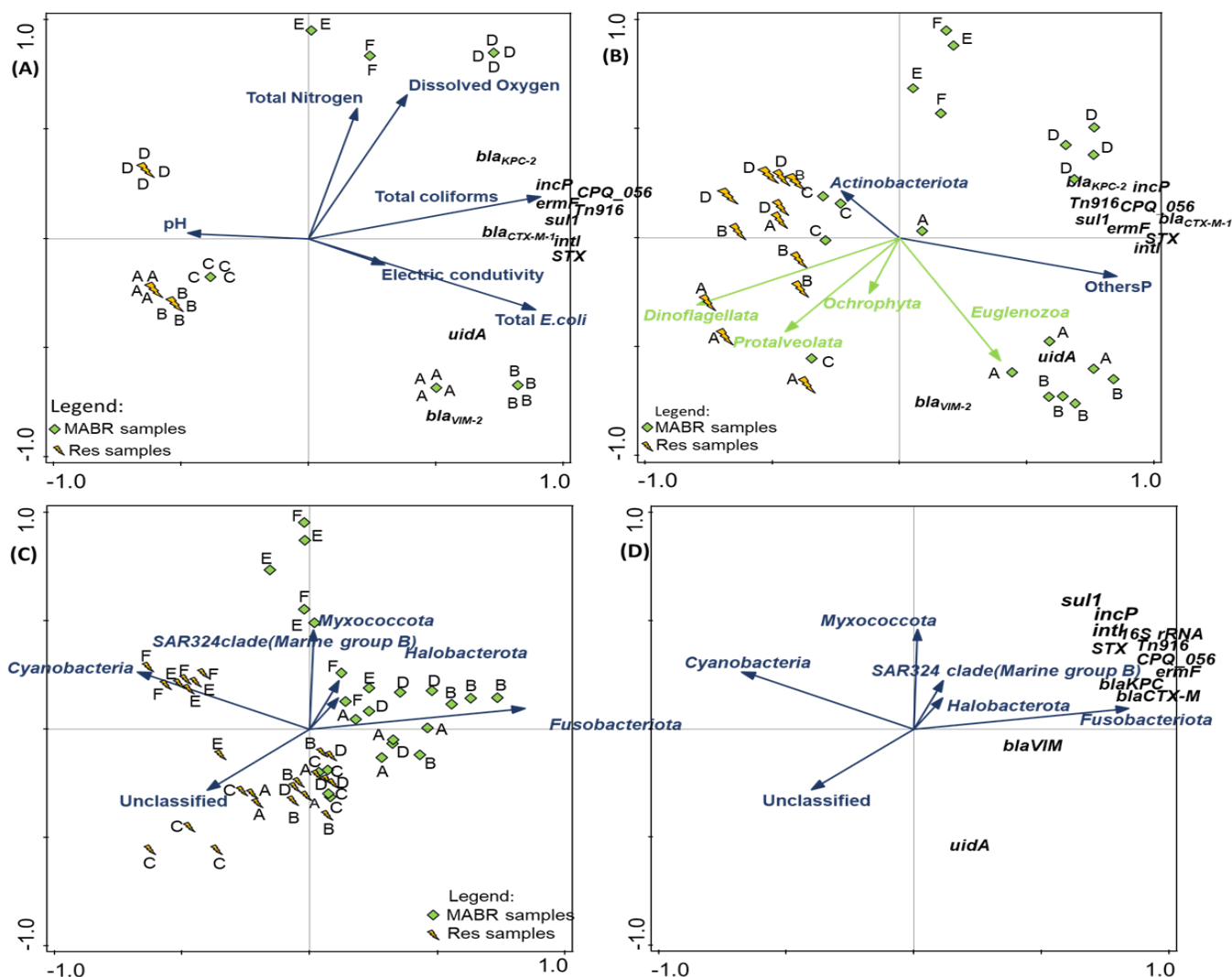
Figure 6. Taxa with significant variations in relative abundances between MABR and reservoir samples. Prokaryotic (A, B) and Eukaryotic communities (C, D), at Class (A, C) and Family (B, D) taxonomic levels. Only the ten most abundant taxa with a significance of p<0.01 are shown.

Assessing correlations between microbial, physiochemical and environmental parameters

Redundancy analysis (RDA) was conducted to investigate possible statistically significant correlations (p< 0.01) between physicochemical parameters, ARGs and MGEs, and the microbial community composition in the raw sewage, MABR and reservoir (**Figure. 7**, **Figure. S8**, **Figure. S9**). Since bacterial and ARG and MGE marker removal in the MABR was at least partially associated with biomass removal, we focused on trends that occurred between the MABR and the reservoir. While correlation does not necessarily indicate causation, we observed trends that potentially shed light on the complex abiotic and biotic processes that occur in the two modules and how they affect the system dynamics. The reduction of

total bacteria observed in the reservoir (as measured by 16S rRNA gene abundance), total coliforms, total *Escherichia coli* (including *uid*A), and all the measured ARGs (except *bla*$_{VIM-2}$) and MGEs was positively correlated (p< 0.01) to pH, and negatively correlated to electric conductivity, total nitrogen and dissolved oxygen. The photosynthetic eukaryotic taxa *Dinoflagellata*, *Proteoalveolata* and *Ochrophyta* strongly correlated (p< 0.01) to the reservoir, as did the bacterial phylum *Actinobacteriota*. In contrast, the non-photosynthetic *Euglenozoa* were significantly associated (p< 0.01) with the MABR.

Figure 7. Redundancy analysis (RDA) of the variation of ARGs, MGEs and prokaryotic and eukaryotic populations in the MABR and reservoir samples. Sampling dates from A to F: A – August 19th, B – August 25th , C – September 15th , D – November 24th , E – December 1st and F – December 15th. (A) – RDA of the variation ARGs, MGEs and uidA gene in MABR (M) and reservoir (R) samples in function of measured physico-chemical parameters. The test variables (ARGs, MGEs and uidA) are represented in black and the explanatory variables in blue (physico-chemical parameters). (B) - RDA of the variation ARGs, MGEs and uidA gene in function of the prokaryotic and eukaryotic community phyla members with relative abundance >5% and >1%, respectively. Additional information and statistical analyses are provided in Table S9. (C) and (D) - Redundancy analysis (RDA) of the variation ARGs, MGEs and 16S rRNA genes in M and

403   R samples in function of prokaryotic community. The test variables (ARGs, MGEs and uidA) are represented
404   in black and the explanatory (prokaryotes) in blue. The explanatory variables were associated with 74.4% of
405   the observed variation among the test variables.

406

Discussion

408   Fecal-derived ARB and associated ARG/MGEs released to aquatic ecosystems from WWTP effluents can
409   contribute to both the local and global scope of antibiotic resistance. Nonetheless, the complexity of receiving
410   aquatic ecosystems prevents holistic understanding of the dynamics and fate of ARB and ARGs in these
411   environments, due to their complexity, varying rates of dilution, and the influx of multiple anthropogenic
412   sources. Bench-scale experiments that apply synthetic wastewater can isolate specific factors that influence
413   antibiotic resistance determinants in WWTPs and receiving environments (35, 36), but may not accurately
414   predict large-scale processes that occur under "real life" environmental conditions. While the pilot reservoir
415   investigated here is not completely representative of large-scale effluent stabilization reservoirs or natural
416   effluent-receiving limnological ecosystems, its size, controlled and contained structure, and influx of real
417   secondary effluents, provided novel insights into the fate and dynamics of ARB and ARGs in aquatic
418   ecosystems receiving WWTP effluents.

419   Raw sewage entering the MABR was uniform, microaerophilic and contained high levels of total
420   nitrogen (primarily ammonia) and organic carbon. Aeration in the MABR increased oxygen levels,
421   facilitating a sharp reduction in dissolved organic matter (and turbidity) and total nitrogen, which was
422   attributed to gasification of nitrogen and carbon to N_2 and CO_2 through combined nitrification/denitrification
423   on the MABR membranes.

424   The total and cefotaxime-resistant *E. coli* and ARG and MGE loads in the MABR dropped by
425   approximately 1.5 log units ml^{-1} between sewage and MABR, but we did not observe a significant reduction
426   in the relative abundance (normalized to 16S rRNA gene levels) of *E. coli* or most of the ARG and MGE
427   markers. This is supported by previous studies reporting that the composition of multidrug resistant *E. coli*
428   (37), microbiomes (38) and ARGs (39) in the aqueous phase of secondary WWTP effluents more closely
429   resembles WWTP influent than the activated sludge, albeit at significantly lower loads. To better understand
430   ABR and ARGs dynamics along the sewage WWTP trajectory, future studies need to differentiate between
431   floc/biofilm-associated and aqueous fractions of the raw sewage and secondary effluents to highlight the
432   differences in microbial communities and enable a complete mass balance of carbon and nitrogen in the
433   system. The bacterial community composition of the MABR effluent was generally closer to that of the raw
434   sewage than to the reservoir. Furthermore, the bacterial families found to be enriched in the MABR relative

435   to the reservoir (*i.e. Arcobacteraceae*, *Bacteroidaceae*, *Aeromonadaceae*, *Competibacteraceae*,

436   *Rhodocyclaceae* and *Leptotrichiaceae*) were all found to be ubiquitous to sewage or wastewater treatment

437   plants (40-45). Previous studies have indicated that WWTP influent microbiomes deriving from sewage are

438   significantly different from fecal microbiomes, and the distribution and diversity of bacterial populations in

439   the aqueous phase of sewer pipes are distinct from those of the pipe biofilms (46), and this may be the case

440   in this study as well.

441   The absolute reduction of ARG and MGE markers and *E. coli* in the MABR and stabilization

442   reservoir were similar for the duration of the experiment. However, in contrast to the MABR, in the reservoir

443   the relative abundance of most of these indicators also dropped significantly in contrast to the MABR,

444   implying that the reservoir microbiome harbored a lower percentage of sewage-derived ARB and mobile

445   ARGs. Indeed, amplicon sequencing of 16 and 18S rRNA genes indicated that the reservoir microbiome was

446   significantly different from that of the MABR, with higher abundance of *Pseudomonadota* and

447   *Acidobacteriota*, and differential presence of bacterial and eukaryotic families characteristic of reservoirs

448   and other aquatic ecosystems (47-49) (Ca. Aquilina PeM15, *Microcystaceae* and *Chlorophyceae*). The

449   coupling of 16S and 18S rRNA gene analyses revealed that the sharp increase in *Cyanobacteria* observed in

450   December 2020 was, in essence, chloroplast, predominantly of the green algal family *Chlorophyceae*. It is

451   unclear whether proliferation of these green "blooms" was linked to reduced temperatures in December, to

452   the fact that it took time for these populations to mature, or to other unknown stochastic or deterministic

453   causes. Similar algae blooms were also observed in a previous study that evaluated plankton community

454   changes in a freshwater reservoir amended with treated wastewater effluents (Teltsch et al. 1992). Algal and

455   cyanobacterial blooms can significantly affect water quality and operation of effluent stabilization reservoirs

456   (24, 50, 51), and thus future studies need to identify specific parameters that induce their proliferation.

457   The removal of ARB and ARG markers in the reservoir was supported by a previous study that

458   observed similar trends in a commercial-scale effluent reservoir used for irrigation (13). We accredit this

459   mitigation to ecosystem resilience (52), attributed at least in part to natural attenuation facilitated by abiotic

460   stressors such as solar radiation, oxidative stress, temperature and nutrient limited conditions (24), and a

461   highly resilient "environmental microbiome" that outcompete and prevent colonization of effluent-derived

462   ARB and associated ARGs as previously described (53). Chen *et al.* showed that reduction of microbial

463   diversity exacerbates the spread of antibiotic resistance in soil , highlighting its importance to resilience and

464   resistance of receiving environments towards fecal derived ARB and ARGs. Interestingly, relative reduction

465   in *E. coli* and ARG and MGE levels was relatively stable in the reservoir, despite strong temporal fluctuations

466   in microbial community composition, suggesting functional redundancy of native environmental

467   communities (55). These "native" communities undoubtedly play a role in competitive exclusion of sewage-

derived ARG-harboring bacteria, which is most likely facilitated by a myriad of mechanisms including adaptation to abiotic stressors (*i.e.* radiation, temperature), resource competition and antibiosis. Amplicon sequencing only provides relative abundance values and future studies need to go beyond the community level and into the functional realm in order to pinpoint genes associated with specific characteristics (*i.e.* metabolic pathways, stress related proteins, antibiotics etc.) that facilitate the observed ecological resilience. Furthermore, batch experiments using synthetic communities should be conducted to divulge the relative effects of biotic *vs.* abiotic factors, and assess the capacity of selected population/communities to mitigate specific ARB and ARGs. These should be complemented with relevant Eukaryotic grazers to evaluate the role of predation.

Our results highlight the robust ARB and ARG removal capacity of effluent storage reservoirs, corroborate a previous study which reported that stabilization reservoirs used for effluent storage prior to irrigation removed fecal coliforms by up to five orders of magnitude before chlorination , depending on retention time and operational conditions. Removal rates of ARGs by the reservoir are comparable to more sophisticated disinfection processes such as chlorination (55) and UV (59), suggesting that they may provide a simple and "environmentally sustainable" alternative. The capacity of autochthonous microbiota to hamper the proliferation of invasive bacteria has been increasingly demonstrated and debated in the scientific literature and should be a major research focus on antibiotic resistance combat in the environment (60, 61). Surprisingly, the shift in reservoir retention time (from 21 to 5 days), did not significantly affect its capacity to remove fecal bacteria and ARGs despite shifts in microbial community composition, contrary to previous reports in large-scale stabilization reservoirs (24). A study that evaluated performance of co-digesters treating food waste (62) found that retention times resulted in significant shifts in microbial communities, but similar to our study did not observe significant changes in digester function. These observations may be explained by a phenomenon described as "functional redundancy of microbial composition" (63). In the reservoir, it may stem from the fact that high and low retention times facilitate microbiomes containing taxa that are functionally redundant, or by the fact that both retention times facilitate the same process rate when combined at the community level, despite harboring functionally different taxa. We need to consider that the reservoir was operated under fluctuating "real life" environmental conditions, and therefore, the propositions described above will need to be tested in more controlled systems.

Conclusions

Temporal analysis revealed that both membrane-based secondary municipal sewage treatment and subsequent reservoir storage mitigated antibiotic resistant bacteria and associated ARGs and MGEs. However, in the MABR the phenomenon was primarily facilitated by biomass removal, whereas in the

reservoir it was attributed to shifts in microbial community composition towards a more resilient "environmental" microbiome that seemingly prevents colonization of fecal derived bacteria and associated genes through competitive exclusion associated with ecosystem resilience. Based on these results, we do not only propose the implementation of reservoirs for storing effluents used for irrigation, but also as a means of mitigating fecal bacteria and antibiotic resistance in effluents discharged to aquatic environments, especially in developing regions that lack sophisticated wastewater treatment infrastructure.

Figure captions

Figure 1. Overview of the experimental beta-site.
A.) Schematic diagram of the raw sewage-Membrane Aerated Biofilm Reactor (MABR)-reservoir continuum at the beta-site. Sampling points SWG (raw Sewage), MABR (membrane aerated bioreactor) and RES (reservoir) with RT (reservoir top): Sampling faucet situated at the top 10 cm of the reservoir; RB (reservoir bottom): Sampling faucet situated at the bottom 10 cm of the reservoir. B.) Profile (Left) and aerial photo of the MABR (middle) and reservoir (Right) at the beta-site.

Figure 2. Physicochemical analyses in the raw sewage (blue circles), MABR (red boxes) and reservoir (green triangles). Temperature (A); pH (B); dissolved oxygen (C); total organic carbon (D). Total nitrogen (E); ammonia (F); nitrate (G); nitrite (H).

Figure 3. (A) Absolute and (B) relative abundances of total and cefotaxime-resistant *E. coli* and of 12 ARGs/MGEs markers. . Each data point represents aggregated data collected from six different sampling times and four biological replicates. One-Way ANOVA Test followed by pairwise two sample t-test highlights significant differences. Colors represented different groups: MGE (blue), ARG (green) and bacterial (orange) markers and indicators (CrAssphage with CPQ_056 gene). The boxes indicates the range between the first and third quartile. The top and bottom whiskers of the boxes represent maximum and the minimum values, respectively. The median line divides the box into interquartile range and the cross

532   represents the mean. Each box represent the spread of time point averages (four biological replicates per time
533   point).

534   **Figure 4**. **Bacterial and Eukarya community composition, structure and diversity**.

535   **Figure 4**. **Bacterial and Eukarya community composition, structure and diversity**. Prokaryotic (Left)
536   and Eukaryotic (right) diversity in raw sewage (Swg), MABR and Reservoir (Res) samples. Sampling dates
537   A – August 19th, B – August 25th, C – September 15th, D – November 24th, E – December 1st and F –
538   December 15th.

539

540   **Figure 5. Microbial community composition.** Dominant bacterial (A) and eukaryotic (B) families based
541   on 16S rRNA (V3-V4) and 18S rRNA (V9) gene amplicons, respectively, in the raw sewage (Swg), MABR
542   and reservoir (Res) samples. Only families with relative abundance of >5% and >1% for the bacteria and
543   eukarya, respectively are shown. MGEs and *uidA* gene in function of the prokaryotic and eukaryotic
544   community phyla members with relative abundance >5% and >1%, respectively, and summed as others (E,
545   eukaryote or P, prokaryote) for lower values. Additional information and statistical analyses are provided in
546   **Table S9**. (C) and (D) - Redundancy analysis (RDA) of the variation ARGs, MGEs and 16S rRNA genes in
547   M and R samples in function of prokaryotic community. The test variables (ARGs, MGEs and uidA) are
548   represented in black and the explanatory (prokaryotes) in blue. The explanatory variables were associated
549   with 78.7% of the observed variation among the test variables.

550

551   **Figure 6. Taxa with significant variations in relative abundances between MABR and reservoir**
552   **samples.** Prokaryotic (A, B) and Eukaryotic communities (C, D), at Class (A, C) and Family (B, D)
553   taxonomic levels. Only the ten most abundant taxa with a significance of $p<0.01$ are shown.

554   **Figure 7. Redundancy analysis (RDA) of the variation of ARGs, MGEs and prokaryotic and**
555   **eukaryotic populations in the MABR and reservoir samples.** Sampling dates from A to F: A – August
556   19th, B – August 25th , C – September 15th , D – November 24th , E – December 1st and F – December 15th.
557   (A) – RDA of the variation ARGs, MGEs and uidA gene in MABR (M) and reservoir (R) samples in function
558   of measured physico-chemical parameters. The test variables (ARGs, MGEs and uidA) are represented in
559   black and the explanatory variables in blue (physico-chemical parameters). (B) - RDA of the variation ARGs,
560   MGEs and uidA gene in function of the prokaryotic and eukaryotic community phyla members with relative
561   abundance >5% and >1%, respectively. Additional information and statistical analyses are provided in Table
562   S9. (C) and (D) - Redundancy analysis (RDA) of the variation ARGs, MGEs and 16S rRNA genes in M and
563   R samples in function of prokaryotic community. The test variables (ARGs, MGEs and uidA) are represented

in black and the explanatory (prokaryotes) in blue. The explanatory variables were associated with 74.4% of the observed variation among the test variables.

References

1. Aarestrup FM, Woolhouse MEJ. 2020. Using sewage for surveillance of antimicrobial resistance. Science 367:630-632.
2. Hendriksen RS, Munk P, Njage P, van Bunnik B, McNally L, Lukjancenko O, Röder T, Nieuwenhuijse D, Pedersen SK, Kjeldgaard J, Kaas RS, Clausen PTLC, Vogt JK, Leekitcharoenphon P, van de Schans MGM, Zuidema T, de Roda Husman AM, Rasmussen S, Petersen B, Bego A, Rees C, Cassar S, Coventry K, Collignon P, Allerberger F, Rahube TO, Oliveira G, Ivanov I, Vuthy Y, Sopheak T, Yost CK, Ke C, Zheng H, Baisheng L, Jiao X, Donado-Godoy P, Coulibaly KJ, Jergović M, Hrenovic J, Karpíšková R, Villacis JE, Legesse M, Eguale T, Heikinheimo A, Malania L, Nitsche A, Brinkmann A, Saba CKS, Kocsis B, Solymosi N, et al. 2019. Global monitoring of antimicrobial resistance based on metagenomics analyses of urban sewage. Nature Communications 10:1124.
3. Pärnänen KMM, Narciso-da-Rocha C, Kneis D, Berendonk TU, Cacace D, Do TT, Elpers C, Fatta-Kassinos D, Henriques I, Jaeger T, Karkman A, Martinez JL, Michael SG, Michael-Kordatou I, O'Sullivan K, Rodriguez-Mozaz S, Schwartz T, Sheng H, Sørum H, Stedtfeld RD, Tiedje JM, Giustina SVD, Walsh F, Vaz-Moreira I, Virta M, Manaia CM. 2019. Antibiotic resistance in European wastewater treatment plants mirrors the pattern of clinical antibiotic resistance prevalence. Science Advances 5:eaau9124.
4. Bürgmann H, Frigon D, W HG, C MM, Pruden A, Singer AC, B FS, Zhang T. 2018. Water and sanitation: an essential battlefront in the war on antimicrobial resistance. FEMS Microbiol Ecol 94.
5. Marano RBM, Fernandes T, Manaia CM, Nunes O, Morrison D, Berendonk TU, Kreuzinger N, Tenson T, Corno G, Fatta-Kassinos D, Merlin C, Topp E, Jurkevitch E, Henn L, Scott A, Heß S, Slipko K, Laht M, Kisand V, Di Cesare A, Karaolia P, Michael SG, Petre AL, Rosal R, Pruden A, Riquelme V, Agüera A, Esteban B, Luczkiewicz A, Kalinowska A, Leonard A, Gaze WH, Adegoke AA, Stenstrom TA, Pollice A, Salerno C, Schwermer CU, Krzeminski P, Guilloteau H, Donner E, Drigo B, Libralato G, Guida M, Bürgmann H, Beck K, Garelick H, Tacão M, Henriques I, Martínez-Alcalá I, Guillén-Navarro JM, et al. 2020. A global multinational survey of cefotaxime-resistant coliforms in urban wastewater treatment plants. Environment International 144:106035.
6. Manaia CM, Rocha J, Scaccia N, Marano R, Radu E, Biancullo F, Cerqueira F, Fortunato G, Iakovides IC, Zammit I, Kampouris I, Vaz-Moreira I, Nunes OC. 2018. Antibiotic resistance in wastewater treatment plants: Tackling the black box. Environ Int 115:312-324.
7. Gurung K, Ncibi MC, Fontmorin J-M, Särkkä H, Sillanpää M. 2016. Incorporating Submerged MBR in Conventional Activated Sludge Process for Municipal Wastewater Treatment: A Feasibility and Performance Assessment. Journal of Membrane Science & Technology 6.
8. Krzeminski P, Tomei MC, Karaolia P, Langenhoff A, Almeida CMR, Felis E, Gritten F, Andersen HR, Fernandes T, Manaia CM, Rizzo L, Fatta-Kassinos D. 2019. Performance of secondary wastewater treatment methods for the removal of contaminants of emerging concern implicated in crop uptake and antibiotic resistance spread: A review. Science of The Total Environment 648:1052-1081.
9. Tong J, Tang A, Wang H, Liu X, Huang Z, Wang Z, Zhang J, Wei Y, Su Y, Zhang Y. 2019. Microbial community evolution and fate of antibiotic resistance genes along six different full-scale municipal wastewater treatment processes. Bioresour Technol 272:489-500.
10. Czekalski N, Sigdel R, Birtel J, Matthews B, Bürgmann H. 2015. Does human activity impact the natural antibiotic resistance background? Abundance of antibiotic resistance genes in 21 Swiss lakes. Environment International 81:45-55.

613 11. Chu BTT, Petrovich ML, Chaudhary A, Wright D, Murphy B, Wells G, Poretsky R, Löffler FE. 2018.
614   Metagenomics Reveals the Impact of Wastewater Treatment Plants on the Dispersal of
615   Microorganisms and Genes in Aquatic Sediments. Applied and Environmental Microbiology
616   84:e02168-17.
617 12. Cacace D, Fatta-Kassinos D, Manaia CM, Cytryn E, Kreuzinger N, Rizzo L, Karaolia P, Schwartz
618   T, Alexander J, Merlin C, Garelick H, Schmitt H, de Vries D, Schwermer CU, Meric S, Ozkal CB,
619   Pons M-N, Kneis D, Berendonk TU. 2019. Antibiotic resistance genes in treated wastewater and in
620   the receiving water bodies: A pan-European survey of urban settings. Water Research 162:320-
621   330.
622 13. Marano RBM, Zolti A, Jurkevitch E, Cytryn E. 2019. Antibiotic resistance and class 1 integron gene
623   dynamics along effluent, reclaimed wastewater irrigated soil, crop continua: elucidating potential
624   risks and ecological constraints. Water Research 164:114906.
625 14. Galvin S, Boyle F, Hickey P, Vellinga A, Morris D, Cormican M. 2010. Enumeration and
626   Characterization of Antimicrobial-Resistant Escherichia coli Bacteria in Effluent from Municipal,
627   Hospital, and Secondary Treatment Facility Sources. Applied and Environmental Microbiology
628   76:4772-4779.
629 15. Karkman A, Do TT, Walsh F, Virta MPJ. 2018. Antibiotic-Resistance Genes in Waste Water.
630   Trends in Microbiology 26:220-228.
631 16. Berendonk TU, Manaia CM, Merlin C, Fatta-Kassinos D, Cytryn E, Walsh F, Bürgmann H, Sørum
632   H, Norström M, Pons M-N, Kreuzinger N, Huovinen P, Stefani S, Schwartz T, Kisand V, Baquero
633   F, Martinez JL. 2015. Tackling antibiotic resistance: the environmental framework. Nature Reviews
634   Microbiology 13:310-317.
635 17. Noble RT, Moore DF, Leecaster MK, McGee CD, Weisberg SB. 2003. Comparison of total
636   coliform, fecal coliform, and enterococcus bacterial indicator response for ocean recreational water
637   quality testing. Water Research 37:1637-1643.
638 18. Garner E, Organiscak M, Dieter L, Shingleton C, Haddix M, Joshi S, Pruden A, Ashbolt NJ,
639   Medema G, Hamilton KA. 2021. Towards risk assessment for antibiotic resistant pathogens in
640   recycled water: a systematic review and summary of research needs. Environ Microbiol 23:7355-
641   7372.
642 19. Alcock BP, Raphenya AR, Lau TTY, Tsang KK, Bouchard M, Edalatmand A, Huynh W, Nguyen A-
643   LV, Cheng AA, Liu S, Min SY, Miroshnichenko A, Tran H-K, Werfalli RE, Nasir JA, Oloni M,
644   Speicher DJ, Florescu A, Singh B, Faltyn M, Hernandez-Koutoucheva A, Sharma AN, Bordeleau
645   E, Pawlowski AC, Zubyk HL, Dooley D, Griffiths E, Maguire F, Winsor GL, Beiko RG, Brinkman
646   FSL, Hsiao WWL, Domselaar GV, McArthur AG. 2019. CARD 2020: antibiotic resistome
647   surveillance with the comprehensive antibiotic resistance database. Nucleic Acids Research
648   48:D517-D525.
649 20. Zhang A-N, Gaston JM, Dai CL, Zhao S, Poyet M, Groussin M, Yin X, Li L-G, van Loosdrecht
650   MCM, Topp E, Gillings MR, Hanage WP, Tiedje JM, Moniz K, Alm EJ, Zhang T. 2021. An omics-
651   based framework for assessing the health risk of antimicrobial resistance genes. Nature
652   Communications 12:4765.
653 21. Paulus GK, Hornstra LM, Medema G. 2020. International tempo-spatial study of antibiotic
654   resistance genes across the Rhine river using newly developed multiplex qPCR assays. Science of
655   The Total Environment 706:135733.
656 22. Czekalski N, Gascón Díez E, Bürgmann H. 2014. Wastewater as a point source of antibiotic-
657   resistance genes in the sediment of a freshwater lake. The ISME Journal 8:1381-1390.
658 23. Eckert EM, Di Cesare A, Coci M, Corno G. 2018. Persistence of antibiotic resistance genes in
659   large subalpine lakes: the role of anthropogenic pollution and ecological interactions. Hydrobiologia
660   824:93-108.
661 24. Friedler E, Juanico M, Shelef G. 2003. Simulation model of wastewater stabilization reservoirs.
662   Ecological Engineering 20:121-145.
663 25. Juanico M, Shelef G. 1991. The Performance of Stabilization Reservoirs as a Function of Design
664   and Operation Parameters. Water Science and Technology 23:1509-1516.
665 26. Rodríguez-Baño J, Picón E, Navarro MD, López-Cerero L, Pascual Á. 2012. Impact of changes in
666   CLSI and EUCAST breakpoints for susceptibility in bloodstream infections due to extended-
667   spectrum β-lactamase-producing Escherichia coli. Clinical Microbiology and Infection 18:894-900.

668 27. Kornspan D, Brendebach H, Hofreuter D, Mathur S, Blum SE, Fleker M, Bardenstein S, Al Dahouk
669   S. 2021. Protein Biomarker Identification for the Discrimination of Brucella melitensis Field Isolates
670   From the Brucella melitensis Rev.1 Vaccine Strain by MALDI-TOF MS. Front Microbiol 12:712601.
671 28. Magoč T, Salzberg SL. 2011. FLASH: fast length adjustment of short reads to improve genome
672   assemblies. Bioinformatics 27:2957-63.
673 29. Wang Q, Garrity GM, Tiedje JM, Cole JR. 2007. Naive Bayesian classifier for rapid assignment of
674   rRNA sequences into the new bacterial taxonomy. Appl Environ Microbiol 73:5261-7.
675 30. Medlin L, Elwood HJ, Stickel S, Sogin ML. 1988. The characterization of enzymatically amplified
676   eukaryotic 16S-like rRNA-coding regions. Gene 71:491-499.
677 31. Chen S, Zhou Y, Chen Y, Gu J. 2018. fastp: an ultra-fast all-in-one FASTQ preprocessor.
678   Bioinformatics 34:i884-i890.
679 32. Rognes T, Flouri T, Nichols B, Quince C, Mahé F. 2016. VSEARCH: a versatile open source tool
680   for metagenomics. PeerJ 4:e2584.
681 33. Caporaso JG, Kuczynski J, Stombaugh J, Bittinger K, Bushman FD, Costello EK, Fierer N, Peña
682   AG, Goodrich JK, Gordon JI, Huttley GA, Kelley ST, Knights D, Koenig JE, Ley RE, Lozupone CA,
683   McDonald D, Muegge BD, Pirrung M, Reeder J, Sevinsky JR, Turnbaugh PJ, Walters WA,
684   Widmann J, Yatsunenko T, Zaneveld J, Knight R. 2010. QIIME allows analysis of high-throughput
685   community sequencing data. Nat Methods 7:335-6.
686 34. Šmilauer P, Lepš J. 2014. Multivariate Analysis of Ecological Data using CANOCO 5, 2 ed
687   doi:DOI: 10.1017/CBO9781139627061. Cambridge University Press, Cambridge.
688 35. Slipko K, Marano RBM, Cytryn E, Merkus V, Wögerbauer M, Krampe J, Jurkevitch E, Kreuzinger
689   N. 2021. Effects of subinhibitory quinolone concentrations on functionality, microbial community
690   composition, and abundance of antibiotic resistant bacteria and qnrS in activated sludge. Journal
691   of Environmental Chemical Engineering 9:104783.
692 36. Stepanauskas R, Glenn TC, Jagoe CH, Tuckfield RC, Lindell AH, King CJ, McArthur JV. 2006.
693   Coselection for microbial resistance to metals and antibiotics in freshwater microcosms.
694   Environmental Microbiology 8:1510-1514.
695 37. Mahfouz N, Caucci S, Achatz E, Semmler T, Guenther S, Berendonk TU, Schroeder M. 2018. High
696   genomic diversity of multi-drug resistant wastewater Escherichia coli. Scientific Reports 8:8928.
697 38. Quintela-Baluja M, Abouelnaga M, Romalde J, Su J-Q, Yu Y, Gomez-Lopez M, Smets B, Zhu Y-G,
698   Graham DW. 2019. Spatial ecology of a wastewater network defines the antibiotic resistance
699   genes in downstream receiving waters. Water Research 162:347-357.
700 39. McConnell MM, Truelstrup Hansen L, Jamieson RC, Neudorf KD, Yost CK, Tong A. 2018.
701   Removal of antibiotic resistance genes in two tertiary level municipal wastewater treatment plants.
702   Science of The Total Environment 643:292-300.
703 40. Venâncio I, Luís Â, Domingues F, Oleastro M, Pereira L, Ferreira S. 2022. The Prevalence of
704   Arcobacteraceae in Aquatic Environments: A Systematic Review and Meta-Analysis. Pathogens.
705   11(2):doi:10.3390/pathogens11020244.
706 41. Newton Ryan J, McLellan Sandra L, Dila Deborah K, Vineis Joseph H, Morrison Hilary G, Eren
707   AM, Sogin Mitchell L. 2015. Sewage Reflects the Microbiomes of Human Populations. mBio
708   6:e02574-14.
709 42. McLellan SL, Huse SM, Mueller-Spitz SR, Andreishcheva EN, Sogin ML. 2010. Diversity and
710   population structure of sewage-derived microorganisms in wastewater treatment plant influent.
711   Environmental Microbiology 12:378-392.
712 43. Shanks Orin C, Newton Ryan J, Kelty Catherine A, Huse Susan M, Sogin Mitchell L, McLellan
713   Sandra L. 2013. Comparison of the Microbial Community Structures of Untreated Wastewaters
714   from Different Geographic Locales. Applied and Environmental Microbiology 79:2906-2913.
715 44. Brand Veronica R, Crosby Laurel D, Criddle Craig S. 2019. Niche Differentiation among Three
716   Closely Related Competibacteraceae Clades at a Full-Scale Activated Sludge Wastewater
717   Treatment Plant and Putative Linkages to Process Performance. Applied and Environmental
718   Microbiology 85:e02301-18.
719 45. Lu H, Chandran K, Stensel D. 2014. Microbial ecology of denitrification in biological wastewater
720   treatment. Water Research 64:237-254.
721 46. McLellan SL, Roguet A. 2019. The unexpected habitat in sewer pipes for the propagation of
722   microbial communities and their imprint on urban waters. Current Opinion in Biotechnology 57:34-
723   41.

724 47. Tandon K, Baatar B, Chiang P-W, Dashdondog N, Oyuntsetseg B, Tang S-L. 2020. A Large-Scale
725   Survey of the Bacterial Communities in Lakes of Western Mongolia with Varying Salinity Regimes.
726   Microorganisms. 8(11):doi:10.3390/microorganisms8111729.
727 48. Komárek J. 2016. Review of the cyanobacterial genera implying planktic species after recent
728   taxonomic revisions according to polyphasic methods: state as of 2014. Hydrobiologia 764:259-
729   270.
730 49. Visser PM, Ibelings BW, Bormans M, Huisman J. 2016. Artificial mixing to control cyanobacterial
731   blooms: a review. Aquatic Ecology 50:423-441.
732 50. Wallace J, Champagne P, Hall G. 2016. Multivariate statistical analysis of water chemistry
733   conditions in three wastewater stabilization ponds with algae blooms and pH fluctuations. Water
734   Research 96:155-165.
735 51. Beran B, Kargi F. 2005. A dynamic mathematical model for wastewater stabilization ponds.
736   Ecological Modelling 181:39-57.
737 52. Sasaki T, Furukawa T, Iwasaki Y, Seto M, Mori AS. 2015. Perspectives for ecosystem
738   management based on ecosystem resilience and ecological thresholds against multiple and
739   stochastic disturbances. Ecological Indicators 57:395-408.
740 53. Orland C, Emilson EJS, Basiliko N, Mykytczuk NCS, Gunn JM, Tanentzap AJ. 2019. Microbiome
741   functioning depends on individual and interactive effects of the environment and community
742   structure. The ISME Journal 13:1-11.
743 54. Chen Q-L, An X-L, Zheng B-X, Gillings M, Peñuelas J, Cui L, Su J-Q, Zhu Y-G. 2019. Loss of soil
744   microbial diversity exacerbates spread of antibiotic resistance. Soil Ecology Letters 1:3-13.
745 55. Narciso-da-Rocha C, Rocha J, Vaz-Moreira I, Lira F, Tamames J, Henriques I, Martinez JL,
746   Manaia CM. 2018. Bacterial lineages putatively associated with the dissemination of antibiotic
747   resistance genes in a full-scale urban wastewater treatment plant. Environ Int 118:179-188.
748 56. Quinteira S, Ferreira H, Peixe L. 2005. First isolation of blaVIM-2 in an environmental isolate of
749   Pseudomonas pseudoalcaligenes. Antimicrobial agents and chemotherapy 49:2140-2141.
750 57. Hubeny J, Korzeniewska E, Buta-Hubeny M, Zieliński W, Rolbiecki D, Harnisz M. 2022.
751   Characterization of carbapenem resistance in environmental samples and Acinetobacter spp.
752   isolates from wastewater and river water in Poland. Science of The Total Environment
753   822:153437.
754 58. Juanico M. 1996. The performance of batch stabilization reservoirs for wastewater treatment,
755   storage and reuse in Israel. Water Science and Technology 33:149-159.
756 59. Wen Q, Yang L, Duan R, Chen Z. 2016. Monitoring and evaluation of antibiotic resistance genes in
757   four municipal wastewater treatment plants in Harbin, Northeast China. Environ Pollut 212:34-40.
758 60. Nnadozie CF, Odume ON. 2019. Freshwater environments as reservoirs of antibiotic resistant
759   bacteria and their role in the dissemination of antibiotic resistance genes. Environ Pollut
760   254:113067.
761 61. Ribeirinho-Soares S, Moreira NFF, Graça C, Pereira MFR, Silva AMT, Nunes OC. 2022.
762   Overgrowth control of potentially hazardous bacteria during storage of ozone treated wastewater
763   through natural competition. Water Research 209:117932.
764 62. Wang C, Wang Y, Wang Y, Cheung K-k, Ju F, Xia Y, Zhang T. 2020. Genome-centric microbiome
765   analysis reveals solid retention time (SRT)-shaped species interactions and niche differentiation in
766   food waste and sludge co-digesters. Water Research 181:115858.
767 63. Allison SD, Martiny JBH. 2008. Resistance, resilience, and redundancy in microbial communities.
768   Proceedings of the National Academy of Sciences 105:11512-11519.
769

770